



Assignments of Bending Vibrations of Ammonia Adsorbed on Solid Surfaces

Journal:	<i>Catalysis Letters</i>
Manuscript ID:	Draft
Manuscript Type:	Original Manuscript
Date Submitted by the Author:	n/a
Complete List of Authors:	Suganuma, Satoshi; Tottori University, Center for Research on Green Sustainable Chemistry, Graduate School of Engineering Murakami, Yuta; Tottori University, Department of Chemistry and Biotechnology, Graduate School of Engineering Ohyama, Jota; Tottori University, Department of Chemistry and Biotechnology, Graduate School of Engineering Torikai, Tatsuya; MicrotracBEL Corp., Okumura, Kazu; Kogakuin University, Department of Applied Chemistry, Faculty of Engineering Katada, Naonobu; Tottori University, Department of Chemistry and Biotechnology, Graduate School of Engineering
Keywords:	Heterogeneous catalysis < Catalysis, Thermal desorption < Elementary Kinetics, Characterization < Methodology and Phenomena, (FT)IR < Microscopy, Spectroscopy and General Characterisation, Mass Spectrometry < Microscopy, Spectroscopy and General Characterisation, Acid catalysis < Processes and Reactions, DFT < Theory

SCHOLARONE™
Manuscripts

Assignments of Bending Vibrations of Ammonia Adsorbed on Solid Surfaces

Satoshi Suganuma*¹, Yuta Murakami², Jota Ohyama², Tatsuya Torikai³, Kazu Okumura⁴, and Naonobu Katada²

¹ Center for Research on Green Sustainable Chemistry, Graduate School of Engineering, Tottori University, 4-101 Koyama-cho Minami, Tottori 680-8552, Japan

² Department of Chemistry and Biotechnology, Graduate School of Engineering, Tottori University, 4-101 Koyama-cho Minami, Tottori 680-8552, Japan

³ MicrotracBEL Corp., 1-1-9 Harada-naka, Toyonaka 561-0807, Japan

⁴ Department of Applied Chemistry, Faculty of Engineering, Kogakuin University, 2665-1 Nakano, Hachioji, Tokyo 192-0015, Japan

* E-mail: suganuma@chem.tottori-u.ac.jp

Abstract

Bending vibrations in the infrared (IR) spectra of ammonia adsorbed on Lewis acidic metal oxides, i.e., Al₂O₃, ZrO₂ and TiO₂, and zeolite were analyzed with an aid of density functional theory (DFT) calculations. The results by DFT methods reveal the wavenumbers of the vibration modes (ν_4 and ν_2) of NH₄ bonded to Brønsted acid site and the vibration modes (δ_s and δ_d) of NH₃ species coordinated to a Lewis acidic metal center (M = Al, Zr or Ti). The wavenumbers calculated based on DFT were reasonably in agreement with the experimentally observed values. The estimation of wavenumbers suggests that the δ_s vibration of NH₃ hydrogen-bonded is invisible on a zeolite, because it is hidden by an intense absorption due to skeletal vibration. On the other hand, multiple bands of asymmetric bending modes (δ_d and ν_2) observed on a zeolite were assigned. A quantification method of Brønsted and Lewis acid sites, and hydrogen-bonded NH₃ is provided based on the peak assignments.

Introduction

Ammonia is a gaseous base compound with a small molecular size and therefore widely utilized as a probe for the characterization of acid sites on solid catalysts and other functional materials. It has been known that, by the adsorption of ammonia, an ammonium cation (NH_4^+) is formed on a Brønsted acid site, a coordinated NH_3 species is formed on a Lewis acid site (metal center), and a hydrogen-bonded (or interacted via specifically strong physical adsorption) NH_3 species is formed on polar species such as Si-OH and NH_4^+ which has been adsorbed on a Brønsted acid site on solid surfaces [1,2]. The NH_3 molecule hydrogen-bonded to NH_4^+ can be expressed as N_2H_7^+ as proposed [3]. Hereafter these three species, NH_4^+ bonded to Brønsted acid site, NH_3 coordinated to Lewis acid site and NH_3 hydrogen-bonded, are termed NH_4B , NH_3L and NH_3H , respectively.

Frequencies or wavenumbers in infrared (IR) spectra of the bending vibrations shown in Figure 1 [4] are the keys to identify the adsorbed species as well as the type of adsorption sites. In a low wavenumber region ($1100 - 1500 \text{ cm}^{-1}$), δ_s of NH_3 and ν_4 of NH_4 can be observed, while δ_d of NH_3 and ν_2 of NH_4 should appear in a high wavenumber region ($1600 - 1800 \text{ cm}^{-1}$). The δ_s of NH_3 and ν_4 of NH_4 modes are termed symmetric vibrations, whereas the δ_d of NH_3 and ν_2 of NH_4 modes are shown as asymmetric vibrations in this paper based on their nature, although the former vibrations are not properly symmetric in some structure.

Niwa et al. developed a method of ammonia IRMS (infrared-mass spectroscopic)-TPD (temperature-programmed desorption) for measurements of the number, strength (enthalpy or energy of ammonia desorption) and type (Brønsted or Lewis) of acid sites on solids [5]. The identification of Brønsted and Lewis acid site is carried out based on the bending frequencies. Practical analysis of the IR spectrum of adsorbed ammonia on a solid sometimes however faces unclear assignments of the bands. Figure 2 shows an example of the temperature dependence of IR spectrum of ammonia adsorbed on a zeolite. Two bands, presumably assigned to symmetric

1 vibrations (δ_s of NH_3 and ν_4 of NH_4), are observed at 1324 and 1444 cm^{-1} . The latter should be
2 ascribed to the ν_4 mode of NH_4B . The former is assigned to any of NH_3L or NH_3H , but further
3 information has not been available. In addition, three bands are found at 1627, 1675 and 1760 cm^{-1} .
4 The assignments have not been established. It is naturally speculated that the three bands are
5 ascribed to possible three asymmetric modes, i.e., ν_2 of NH_4B , and δ_d of NH_3L and NH_3H . It is
6 difficult to answer to the question why the symmetric (δ_s and ν_4) vibrations reveal the presence of
7 two species while the asymmetric (δ_d and ν_2) vibrations suggest the presence of three species. On
8 the other hand, the intensities of these bands are decreased with elevating the temperature. The
9 band at 1675 cm^{-1} was almost completely diminished at a relatively low temperature compared to
10 the other asymmetric bands, suggesting the relation of this band to hydrogen bond with a relatively
11 weak interaction. However, the corresponding symmetric band diminishing at a low temperature is
12 not observed in the spectrum.
13
14
15
16
17
18
19
20
21
22
23
24
25
26
27

28 The aim of this study is to give answers to these questions and to establish the assignments
29 of these vibration bands in order to make possible to quantify each of adsorbed species of ammonia.
30 Theoretical study has been attempted to interpret the vibrations of adsorbed ammonia species in
31 zeolite micropores [3,6]. Density functional theory (DFT) [7] is utilized to estimate the vibration
32 frequencies of related species over Lewis acidic metal oxides such as Al_2O_3 and ZrO_2 as well as on
33 the zeolite in this study. The calculated wavenumber values are compared to the experimentally
34 observed wavenumbers in order to assign the experimentally observed vibrations. It should be
35 noted that the assignment of symmetric vibration of NH_4 bonded to Brønsted acid site, i.e., most
36 important species to interpret the Brønsted acidity, has been established and analyzed theoretically
37 [3,6]. The discussion is focused on the unsolved problems as above.
38
39
40
41
42
43
44
45
46
47
48
49
50

51 Method

52 1. Experimental

1
2 The employed metal oxides, and USY (ultrastable Y) and MOR (mordenite) zeolites are
3 shown in Table 1. The preparation of TiO₂ was according to Cao et al. [8], while the USY zeolite
4 was prepared as described in our previous paper [9].
5
6
7

8 Ammonia IRMS-TPD analysis was carried out using an automatic IRMS-TPD analyzer
9 (MicrotracBEL, Japan). The measurement conditions referred to our previous paper, in which
10 homemade IRMS-TPD analyzer was used [10]. About 7 mg of the sample was compressed into a
11 self-supporting disk with 1 cm of the diameter under 20 MPa, and pre-treated in an oxygen flow (37
12 μmol s⁻¹, 100 kPa) at 823 K for 1 h in an in-situ IR cell. IR spectra were recorded before and after
13 NH₃ adsorption. The sample was heated at a ramp rate of 2 K min⁻¹ during the elevation
14 temperature from 373 to 823 K in a helium flow (89 μmol s⁻¹, 6.0 kPa), and an IR spectrum was
15 collected before and after ammonia adsorption at an interval of 2 K. The concentration of ammonia
16 in the gas phase was monitored by a mass spectrometer (MS) operating at *m/e* 16.
17
18
19
20
21
22
23
24
25
26
27

28 IR spectra at a constant temperature with varying the coverage were obtained using FT/IR-
29 4200 (JASCO, Japan). The sample was pretreated at 823 K in oxygen for 1 h, and then evacuated at
30 823 K for 1 h. An IR spectrum for the background was measured at 673 K under vacuum. Ammonia
31 was gradually introduced at 673 K. The spectra were collected before the vessel was evacuated and
32 after each evacuation time.
33
34
35
36
37
38

39 2. Theoretical

40 Model clusters containing NH₃ species shown in Table were assumed. Species NH₃→M
41 (M = Al, Zr and Ti) were the employed for modeling NH₃L in entries 1-3. Entry 4, namely, NH₃
42 molecule interacting with an H atom in a silanol group, was adopted for modeling NH₃H.
43
44
45
46
47

48 The structural optimization, calculation of total binding energy and analysis of vibrations
49 were carried out using Dmol³ software (Accelrys Inc.) [11] on a generalized gradient approximation
50 (GGA) level using Becke-Lee-Yang-Parr (BLYP) exchange and correlation functional [12]. All
51 electrons were taken into account as well as the relativistic effect. The calculations were performed
52
53
54
55
56
57
58
59
60

1 using a double numerical polarization (DNP) basis set. The convergence criteria (energy, force and
2 displacement) were set to 2×10^{-5} Ha, 4×10^{-3} Ha \AA^{-1} and 5×10^{-3} \AA , respectively (1 Ha = 4.360×10^{-18} J
3 = 2625 kJ mol⁻¹, 1 \AA = 10^{-10} m).
4
5
6
7
8
9

10 Results

11 1. Experimental

12 Figure 3 shows the IR spectra of three metal oxides employed. The contribution of
13 adsorbed ammonia is shown here by a difference spectrum [(spectrum after the adsorption) -
14 (spectrum before the adsorption)]. Bands attributable to the bending vibrations (δ_s and δ_d) of NH₃L
15 were observed at 1168 and 1599 cm⁻¹, respectively, on TiO₂. The wavenumbers of both bands on
16 ZrO₂, 1173 and 1602 cm⁻¹ for δ_s and δ_d , respectively, were higher than those of the corresponding
17 modes on TiO₂. The wavenumber of δ_s band was further high on Al₂O₃ (1224 cm⁻¹), and in
18 addition to the NH₃L, the band assignable to ν_4 of NH₄B was found at 1466 cm⁻¹. Pure γ -Al₂O₃ is
19 generally believed to have Lewis acidity only, but the presence of weak Brønsted acid sites which
20 could protonate ammonia was reported [13]. We have reported a similar spectrum of ammonia
21 adsorbed on a different sample of γ -Al₂O₃ (a reference catalyst JRC-ALO4) [14]. The asymmetric
22 band on Al₂O₃ seems to be separated into two components, 1624 and 1691 cm⁻¹. These are
23 speculated to be due to NH₃ and NH₄. The assignments of these bands will be discussed with an aid
24 of theoretical study in the next section. Before the complete assignments, one can say that any of
25 the wavenumber of δ_d band on Al₂O₃ was higher than those on ZrO₂ and TiO₂.
26
27
28
29
30
31
32
33
34
35
36
37
38
39
40
41
42
43
44
45

46 Figure 2 shows the IR spectrum of NH₃ adsorbed on the USY zeolite. Several bands were
47 observed as stated in the previous section. The large band at 1444 cm⁻¹ is presumably ascribed to
48 the ν_4 vibration of NH₄ which was formed on the Brønsted acid site. A small band of δ_s vibration of
49 NH₃ was also observed at 1324 cm⁻¹. We have to note that the strong absorption around 1200 cm⁻¹
50 by the Si-O skeleton seems to hide the low wavenumber region of this band. In addition, three
51
52
53
54
55
56
57
58
59
60

bands ascribable to asymmetric vibrations were observed at 1627, 1675 and 1760 cm^{-1} .

The temperature dependence of intensities of the five bands on USY was analyzed according to the IRMS-TPD procedure [10]. The absorption spectrum in the range between 1250 and 1850 cm^{-1} was deconvoluted into the fragments as shown in Figure 4. The differentiation of peak area by temperature ($-dA/dT$ where A and T are the absorbance and temperature, respectively), i.e., IR-TPD profile, was calculated to show the desorption rates of ammonia from the corresponding adsorption sites, as shown in Figure 5. The IR-TPD profile of 1675 cm^{-1} -band shows that the NH_3 desorption had finished at <600 K. The desorption temperature of this 1675 cm^{-1} -band was lowest among the IR-TPD profiles of five bands. From the wavenumber (1675 cm^{-1}), this peak is assigned to asymmetric vibration of some adsorbed species. However, the corresponding desorption peak due to symmetric vibration in the low wavenumber region was not found at the same temperature. The peak temperature of the IR-TPD of 1627 cm^{-1} -band was observed in the next temperature region (420 to 450 K). This peak temperature was similar to that of 1324 cm^{-1} -band. The IR-TPD of 1760 cm^{-1} -band had the broad peak temperature (450 to 500 K) higher than those of 1627 and 1760 cm^{-1} -bands, and similar to that of 1444 cm^{-1} -band.

Figure 6 shows difference IR spectra between the spectra measured after pre-treatment and spectra measured after the ammonia adsorption and evacuation on MOR at 673 K. The MOR has strong Brønsted acid sites comparable to USY, and scarcely any Lewis acid sites [9,10]. The large band at 1430 cm^{-1} was assigned to the ν_4 vibration of NH_4 which was formed on the Brønsted acid site. The peak position of this band was unchanged even after evacuation for 15 hours. The broad band at 1773 cm^{-1} was ascribed to asymmetric vibrations. The sharp peak at 1625 cm^{-1} attributable to gaseous ammonia disappeared immediately after starting evacuation.

2. Theoretical

The structural optimization of assumed clusters was converged into reasonable structures, as the final coordinates are listed in Tables 3 to 8. The wavenumbers calculated are listed in Table .

1 The optimized structure of $\text{H}_3\text{N}\rightarrow\text{Al}(\text{OH})_3$ (entry 1) is shown in Figure 7. The N atom in
2 the NH_3 molecule attaches to Al with a distance of 2.062 Å, indicating that this model can represent
3 the nature of NH_3L . Both wavenumbers of δ_s and δ_d bands gradually shifted higher from entries 1
4 to 3. It tells us that the frequencies of these bands are dependent on the metal to which NH_3 is
5 coordinated as $\text{Al} > \text{Zr} > \text{Ti}$.
6
7
8
9
10
11

12 The optimized structure of $\text{H}_3\text{N}\cdots\text{H}-\text{O}-\text{Si}(\text{OH})_3$ (entry 4) is shown in Figure 8, indicating
13 that the N atom attaches to H with an N-O distance of 2.840 Å, and therefore hydrogen bond exists
14 between the N and H atoms. It is revealed that the hydrogen-bonded species (NH_3H) has 1114 cm^{-1}
15 of δ_s , lower than any of NH_3 species coordinated to Lewis acidic metal centers. On the other hand,
16 the wavenumber of δ_d of this species (1627 cm^{-1}) was higher than those of the Lewis acid-
17 coordinated species.
18
19
20
21
22
23
24
25

26 A free NH_3 molecule (entry 5) is indicated to have further low δ_s and high δ_d
27 wavenumbers. The hydrogen bond, a weaker interaction than the coordination to the Lewis acid
28 center, results in the lower δ_s and higher δ_d than those of NH_3L as above. This is in agreement with
29 the observed trend in entry 5 where the lack of atoms surrounding the NH_3 molecule provides the
30 low δ_s and high δ_d frequencies.
31
32
33
34
35
36

37 Entries 6-9 show that a NH_4^+ cation, formed on a Brønsted acid site, has ν_4 vibrations
38 around 1450 cm^{-1} , as observed on a typical Brønsted acidic solid as zeolite, and a ν_2 vibration at the
39 highest wavenumber.
40
41
42
43
44
45

46 Discussion

47 The δ_s wavenumbers of $\text{H}_3\text{N}\rightarrow\text{M}$ species ($\text{M} = \text{Ti}, \text{Zr}$ or Al) calculated were about 10 to 40
48 cm^{-1} lower than the wavenumbers experimentally observed in the IR spectra of NH_3 adsorbed on
49 the corresponding MO_x , which are listed in Table in order to compare these values.
50
51
52
53
54

55 It is reasonable to assign the 1691 and 1624 cm^{-1} -bands on Al_2O_3 to those of ν_2 of NH_4 and
56
57
58
59
60

1 δ_d of NH_3 , because the DFT calculations show that the free NH_4^+ cation has the highest
2 wavenumber. Subsequently it becomes clear as shown in entries 1-3 (Table) that the δ_d
3 wavenumbers of NH_3L calculated were 4 to 20 cm^{-1} higher than the observed values. The shifts of
4 δ_s and δ_d bands into high wavenumbers from Ti, Zr to Al in the calculated values were also in
5 agreement with the observations. It seems that the present assumptions of small clusters and the
6 DFT calculations approximately demonstrate the important properties of NH_3 species adsorbed on
7 the different metal oxide surfaces.
8

9
10
11
12
13
14
15
16
17 It is estimated from the DFT calculations that NH_3H had 1114 cm^{-1} of the δ_s band.
18 Because the calculated values of NH_3L were about 10 to 40 cm^{-1} lower than those of the observed
19 values as above, the actual wavenumber of NH_3H is suspected to be around 1120 - 1150 cm^{-1} . It is
20 pointed out that the skeletal vibration of zeolite covers the wavenumber region less than 1250 cm^{-1} ,
21 and hence the δ_s vibration of NH_3H at 1120 - 1150 cm^{-1} must be invisible on zeolites. In contrast,
22 the band of NH_3 coordinated to Al around 1250 cm^{-1} is believed to be observed, because the high
23 wavenumber region of this band should not be overlapped by the skeletal vibration. The band at
24 1324 cm^{-1} should be a fraction of the band of NH_3L . It is reasonable to use this intense band δ_s for
25 quantification of the Lewis acid sites, while NH_3H cannot be quantified based on the δ_s vibration on
26 zeolite.
27

28
29
30
31
32
33
34
35
36
37
38
39 Multiple bands of δ_d was observed on Al_2O_3 and USY. The DFT indicates that the
40 asymmetric band should appear in the order of wavenumber as $\text{NH}_3\text{L} < \text{NH}_3\text{H} < \text{NH}_4\text{B}$. The three
41 bands found on USY, i.e., the bands at 1627, 1675 and 1760 cm^{-1} , are therefore assigned to the δ_d
42 vibration of NH_3L and NH_3H , and the ν_2 mode of NH_4B , respectively. The assignment of NH_3H is
43 generally in agreement with the study by Lónyi and Valyon, in which they assigned the IR bands
44 based on the thermal behaviors [15]. The two bands on alumina (1624 and 1691 cm^{-1}) can be
45 assigned to NH_3L and NH_4B , respectively.
46
47
48
49
50
51
52
53

54
55 In order to confirm the former assignments, the temperature dependence of the intensities
56
57
58
59
60

1 of three bands on USY was analyzed. The desorption temperature of the species shown by the band
2 at 1675 cm^{-1} , assigned to NH_3H as above, was in the lowest starting and end temperature region of
3 desorption. No peak with similar desorption temperature was found in the low wavenumber (δ_s)
4 region. Weak interaction is estimated from the low desorption temperature. These are consistent
5 with the attribution of this band to the δ_d mode of NH_3H , and it is confirmed that the corresponding
6 δ_s mode was hidden by the skeletal vibration of silicate.
7
8
9

10 The peak maximum temperature of the IR-TPD of 1760 cm^{-1} -band, assigned to ν_2 of
11 NH_4B , in the broad temperature region (450 to 500 K), and the temperature range was not
12 significantly different from the peak temperature of IR-TPD of the ν_4 vibration of NH_4B (1444
13 cm^{-1}). This is also consistent with the assignment of 1760 cm^{-1} -band to the ν_2 mode of NH_4B . In the
14 IR spectra of MOR at the constant temperature, the bands at 1430 and 1773 cm^{-1} was assigned to
15 the ν_4 vibration and the ν_2 mode of NH_4B , because it has been clear that MOR has strong Brønsted
16 acid sites. These assignments are consistent with different zeolites.
17
18
19
20
21
22
23
24
25
26
27
28
29

30 The IR-TPD of 1627 cm^{-1} -band, attributed to δ_d of NH_3L had the similar peak temperature
31 (420 to 450 K) to that of 1324 cm^{-1} -band, assigned to δ_s of NH_3L . This is in agreement with the
32 above discussion in which these bonds were due to the different modes of one species.
33
34
35
36

37 The three asymmetric bands at 1627 , 1675 and 1760 cm^{-1} on USY have thus been assigned
38 to NH_3 coordinated to Lewis acid site, hydrogen-bonded NH_3 and NH_4^+ bonded to Brønsted acid
39 site. In addition, it is reasonable to quantify the Brønsted acid sites and Lewis acid sites based upon
40 the strong symmetric bands observable at 1444 and 1324 cm^{-1} , respectively, while the quantification
41 of hydrogen-bonded species needs analysis of the small δ_d band at 1675 cm^{-1} .
42
43
44
45
46
47

48 The relationship between MS-TPD, C_g (concentration of ammonia in gas phase), and IR-
49 TPD can be drawn as follows.
50
51
52
53
54
55
56
57
58
59
60

$$C_g = \sum \left\{ \frac{\pi D^2 \beta}{4F \varepsilon_i} \left(-\frac{dA}{dT} \right)_i \right\} \quad (1)$$

where D , β , F , ε_i and $\left(-\frac{dA}{dT} \right)_i$ are the diameter of sample disk, ramp rate, flow rate of carrier gas, molar extinction absorption coefficient of the discussed species and IR-TPD of the discussed species, respectively. The parameter ε_i is specific to the material and vibration mode, and therefore unknown before experiments. We can estimate through curve-fitting procedure of C_g and $\sum \left\{ \frac{\pi D^2 \beta}{4F \varepsilon_i} \left(-\frac{dA}{dT} \right)_i \right\}$ over the temperature range with adjusting the parameters ε_i . The obtained $\frac{\pi D^2 \beta}{4F \varepsilon_i} \left(-\frac{dA}{dT} \right)_i$ should be the ammonia TPD spectrum of each kind of adsorption site.

Figure 9 shows the TPD spectra of NH_4B , NH_3L and NH_3H derived from the IR-TPD of 1444 cm^{-1} -band (ν_4 of NH_4B), 1324 cm^{-1} -band (δ_s of NH_3L) and 1675 cm^{-1} -band (δ_d of NH_3H). It appears that the temperature range of MS-TPD peak was broad, because MS-TPD was the sum of TPD profiles of these three species having different desorption temperature ranges.

The obtained peak area of TPD profile shows the number of each type of adsorption site, whereas the enthalpy or energy of ammonia desorption as an index of adsorption strength can be calculated from the peak area, position and shape [16]. Among them, the numbers and strengths of Brønsted and Lewis acid sites are directly useful for analysis of solid acid catalysis. In contrast, the information from NH_3H should be a noise for the analysis of solid acidic property in most cases. It is believed that separation of the signals due to actual acid sites from the noise is also important. The removal of NH_3H species has been carried out by introduction of water vapor in the conventional technique of ammonia TPD [17-19]. This is owing to the physicochemical nature of ammonia and water; ammonia is a stronger base than water, and therefore ammonia species

1 adsorbed on an acid site cannot be replaced with water, while an NH bond is less polar than an OH
2 bond, and therefore hydrogen-bonded ammonia is replaced with water. A disadvantage of the water
3 introduction can be raised; nature and microstructure of a surface can be changed by water. The
4 identification of the adsorbed species in the IR spectrum achieved in the present study will extend
5 these techniques to more accurate analysis.
6
7
8
9
10
11

12 Conclusions

13 (1) DFT calculations of the NH₃ species coordinated to Lewis acidic metal center gives the
14 reasonable wavenumbers of δ_s and δ_d bands.
15

16 (2) Bending vibrations of ammonia adsorbed on metal oxides and zeolites are assigned with an aid
17 of DFT. As a result, the wavenumbers of δ_s and δ_d vibrations of NH₃ hydrogen-bonded are
18 estimated.
19

20 (3) On a silicate, it is clarified that the δ_s vibration of hydrogen-bonded species is invisible because
21 it is hidden by the skeletal vibration, whereas δ_d of the hydrogen-bonded species can be observed.
22 The other vibrations, i.e., both ν_4 and ν_2 of NH₄ bonded to Brønsted acid site and δ_s and δ_d of NH₃
23 coordinated to Lewis acid site can be observed.
24

25 (4) Quantification of Brønsted and Lewis acid sites, and hydrogen-bonded NH₃ is possible by
26 means of an ammonia IRMS-TPD method based on the above peak assignments.
27

28 Acknowledgement

29 This study was partly supported by a Grant-in-Aid for Scientific Research (B) 23360358
30 from the Ministry of Education, Culture, Sports, Science and Technology, Japan.
31
32
33
34
35
36
37
38
39
40
41
42
43
44
45
46
47
48
49
50
51
52
53
54
55
56
57
58
59
60

-
- 1
2
3
4 [1] Lónyi F, Valyon J (2001) *Thermochim Acta* 373:53.
5
6 [2] Earl WL, Fritz PO, Gibson AAV, Lunsford JH (1987) *J Phys Chem* 91:2091.
7
8 [3] Zecchina A, Marchese L, Bordiga S, Pazé C, Gianotti E (1997) *J Phys Chem B* 101:10128.
9
10 [4] Nakamoto K, *Infrared and Raman Spectra of Inorganic and Coordination Compounds*, 6th
11 edition (John Wiley & Sons, New York, 2009).
12
13 [5] Niwa M, Katada N, Okumura K, *Characterization and Design of Zeolite Catalysts: Solid*
14 *Acidity, Shape Selectivity and Loading Properties* (Springer, Berlin, 2010).
15
16 [6] Bučko T, Hafner J, Benco L (2004) *J Chem Phys* 120:10263.
17
18 [7] Sholl DS, Steckel JA, *Density Functional Theory: A Practical Introduction* (Wiley, Hoboken,
19 2009).
20
21 [8] Cao L, Huang A, Spiess F-J, Suib SL (1999) *J Catal* 188:48.
22
23 [9] Okumura K, Tomiyama T, Morishita N, Sanada T, Kamiguchi K, Katada N, Niwa M (2011)
24 *Appl Catal A: Gen* 405:8.
25
26 [10] Niwa M, Suzuki K, Katada N, Kanougi T, Atoguchi T (2005) *J Phys Chem B* 109:18749.
27
28 [11] Delly B, Ellis DE, Freeman AJ, Baerends EJ, Post D (1983) *Phys Rev B* 27:2132.
29
30 [12] Becke AD (1986) *J Chem Phys* 104:1040.
31
32 [13] Shen Y-F, Suib SL, Deeba M, Koermer GS (1994) *J Catal* 146:483.
33
34 [14] Niwa M, Katada N, Murakami Y (1990) *J Phys Chem* 94:6441.
35
36 [15] Lónyi F, Valyon J (2001) *Micropor Mesopor Mater* 47:293.
37
38 [16] Katada N, Igi H, Kim J-H, Niwa M (1997) *J Phys Chem B* 101:5969.
39
40 [17] Woolery GL, Kuehl GH, Timken HC, Chester AW (1997) *Zeolites* 19:288.
41
42 [18] Bagnasco G (1996) *J Catal* 159:249.
43
44 [19] Igi H, Katada N, Niwa M, *Proceedings of the 12th International Zeolite Conference*, ed. by
45 Treacy MMJ, Marcus BK, Bisher ME, Higgins JB, Materials Research Society, Warrendale, 1999,
46
47
48
49
50
51
52
53
54
55
56
57
58
59
60

pp. 2643-2650.

For Peer Review

1
2
3
4
5
6
7
8
9
10
11
12
13
14
15
16
17
18
19
20
21
22
23
24
25
26
27
28
29
30
31
32
33
34
35
36
37
38
39
40
41
42
43
44
45
46
47
48
49
50
51
52
53
54
55
56
57
58
59
60

Table 1 Employed oxide samples

Description	Origin
Al ₂ O ₃	Reference catalyst JRC-ALO6 supplied by Reference Catalyst Division, Catalysis Society of Japan, as received
ZrO ₂	Hydrolysis of Zr(ONO ₃) ₂ with NH ₄ OH in an aqueous solution followed by calcination at 773 K for 4 h
TiO ₂	Hydrolysis of Ti[OCH(CH ₃) ₂] with H ₂ O in ethanol followed by calcination at 773 K for 4 h [8]
USY	Small particles (diameter < 50 nm) of USY prepared from a commercial sample of NaY zeolite (HSZ-320NAA from Tosoh, SiO ₂ /Al ₂ O ₃ = 5.5) by ion-exchange with NH ₄ NO ₃ , steaming at 823 K with H ₂ O (18 mol%) / N ₂ and treatment with NH ₄ NO ₃ at 353 K [9]
MOR	Ion-exchange of JRC-Z-M15 with Si/Al ₂ = 15 (Reference catalyst, Reference Catalyst Division, Catalysis Society of Japan) with NH ₄ NO ₃ at 353 K.

Table 2 Calculated and observed wavenumbers. All the calculations have been corrected by multiplying with 0.9630, because the OH stretching wavenumber was calculated to be 3798 cm^{-1} under the same conditions while it was observed at 3657 cm^{-1} .

Entry	Description	Wavenumber (cm^{-1}) of			
		$\delta_s(\text{NH}_3)$ or $\nu_4(\text{NH}_4)$		$\delta_d(\text{NH}_3)$ or $\nu_2(\text{NH}_4)$	
		calc.	obs.	calc.	obs.
1	$\text{H}_3\text{N} \rightarrow \text{Al}(\text{OH})_3$	1206	1224 ^a	1602, 1617	1624 ^a
	$\text{H}_3\text{N}/\text{Al}_2\text{O}_3$	1226	1224	1593, 1606	1624
2	$\text{H}_3\text{N} \rightarrow \text{Zr}(\text{OH})_4$	1134	1173 ^b	1566, 1602	1602 ^b
3	$\text{H}_3\text{N} \rightarrow \text{Ti}(\text{OH})_4$	1154	1168 ^c	1592, 1630	1599 ^c
	$\text{H}_3\text{N}/\text{TiO}_2$	1156	1168	1613, 1653	1599
4	$\text{H}_3\text{N} \cdots \text{H}-\text{O}-\text{Si}(\text{OH})_3$	1123		1601, 1615	
5	Free NH_3	1050	1084	1607, 1634	1627
6	$\text{NH}_4 \cdots \text{FAU}$	1319, 1436, 1495	1450 ^d	1640, 1675	1674, 1774
7	$\text{NH}_4 \cdots \text{BEA}$	1344, 1472, 1511	1450 ^d	1673, 1686	1698
8	$\text{NH}_4 \cdots \text{MFI}$	1345, 1473, 1500	1450 ^d	1675, 1676	
9	$\text{NH}_4 \cdots \text{MOR}$		1450 ^d		1582, 1804
10	Free NH_4^+	1430, 1444, 1473		1681, 1694	

a: Observed on Al_2O_3 . b: Observed on ZrO_2 . c: Observed on TiO_2 . d: It looks that a broad band was formed from peaks at 1395 , 1445 and 1490 cm^{-1} .

Table 3 Final coordinates of entry 1, $\text{H}_3\text{N} \rightarrow \text{Al}(\text{OH})_3$ (Å)

ID	ATOM	X	Y	Z
1	N	-4.081580	0.773485	-0.684991
2	Al	-2.421710	-0.000899	0.261624
3	O	-1.463078	1.461537	0.385450
4	O	-1.945003	-1.183342	-0.940260
5	O	-3.209663	-0.585120	1.715469
6	H	-3.895919	1.721776	-1.025207
7	H	-4.871509	0.813296	-0.033480
8	H	-4.352062	0.192178	-1.483844
9	H	-3.068668	-1.504843	1.985993
10	H	-1.036146	-1.165325	-1.275970
11	H	-1.152732	1.738705	1.260736

Table 4 Final coordinates of entry 2, $\text{H}_3\text{N} \rightarrow \text{Zr}(\text{OH})_4$ (Å)

ID	ATOM	X	Y	Z
1	N	-4.168566	0.747810	-1.088112
2	Zr	-2.223629	0.445466	0.507362
3	O	-1.337929	0.855829	-1.268799
4	O	-2.900826	-1.442372	0.656379
5	H	-3.997108	1.611308	-1.610041
6	H	-5.080284	0.836977	-0.633345
7	H	-4.219785	-0.011671	-1.771089
8	H	-3.409282	-1.952950	1.302386
9	H	-0.375092	0.954185	-1.350894
10	O	-0.632334	0.427492	1.721550
11	O	-3.288680	1.931244	1.395828
12	H	-2.968697	2.375267	2.199095
13	H	-0.117290	-0.222984	2.217786

Table 5 Final coordinates of entry 3, $\text{H}_3\text{N} \rightarrow \text{Ti}(\text{OH})_4$ (Å)

ID	ATOM	X	Y	Z
1	N	-4.092437	0.693477	-1.075752
2	Ti	-2.278168	0.467780	0.460448
3	O	-1.374531	0.803940	-1.160820
4	O	-2.836046	-1.306636	0.670554
5	H	-4.293349	1.691254	-1.178703
6	H	-4.956200	0.223519	-0.796682
7	H	-3.804529	0.330606	-1.987766
8	H	-3.312982	-1.616478	1.459563
9	H	-0.413361	0.939213	-1.078482
10	O	-0.836793	0.534933	1.653737
11	O	-3.256497	1.859914	1.266797
12	H	-2.848851	2.216879	2.077195
13	H	-0.415759	-0.282800	1.968012

Table 6 Final coordinates of entry 4: $\text{H}_3\text{N} \cdots \text{H}_a\text{-O-Si}(\text{OH})_3$ (Å)

ID	ATOM	X	Y	Z
1	N	-3.149728	1.931289	3.646233
2	Si	-2.145739	-0.054356	0.422084
3	O	-0.687346	0.748297	0.516893
4	O	-2.609491	-0.289966	-1.153493
5	O	-1.808672	-1.499749	1.203879
6	H	-2.478569	2.703158	3.620246
7	H	-4.046269	2.324543	3.943574
8	H	-2.843868	1.294843	4.386341
9	H	-2.555336	-2.118869	1.261648
10	H	-1.916167	-0.649890	-1.730019
11	H	0.013948	0.231239	0.947003
12	O	-3.394994	0.777003	1.062552
13	H	-3.281645	1.152197	1.982249

Table 7 Final coordinates of entry 5, free NH₃ (Å)

ID	ATOM	X	Y	Z
1	N	-0.010477	-0.014395	0.024595
2	H	-0.316066	-0.446786	-0.852060
3	H	-0.315673	0.961076	-0.039395
4	H	1.010932	0.022475	-0.039001

Table 8 Final coordinates of entry 6, free NH₄⁺ (Å)

ID	ATOM	X	Y	Z
1	N	-0.034779	-0.005575	0.000586
2	H	-0.313716	-0.461686	-0.881707
3	H	-0.324085	0.984404	-0.017597
4	H	0.989452	-0.062860	0.108671
5	H	-0.491362	-0.481867	0.793339

Figure captions

Figure 1: Vibration modes of NH_4 (ammonium cation) and NH_3 coordinated to Lewis acidic metal species. ●, ○ and ● show N, H and M (Lewis acidic metal) atoms, respectively.

Figure 2: Difference IR spectra [(spectrum after measured the ammonia adsorption)-(spectrum before measured the ammonia adsorption)] of USY zeolite recorder at every 10 K during temperature elevation.

Figure 3: Difference IR spectra [(spectrum after measured the ammonia adsorption)-(spectrum before measured the ammonia adsorption)] of (A) Al_2O_3 , (T) TiO_2 and (Z) ZrO_2 .

Figure 4: Deconvolution of IR peaks on USY zeolite at 373 K. L_s and B_s show the assumed bands due to symmetric (δ_s or ν_2) vibration modes of NH_3L and NH_4B , respectively, whereas L_d , H_d and B_d show those due to asymmetric (δ_d or ν_4) modes of NH_3L , NH_3H and NH_4B , respectively.

Figure 5: IR-TPD spectra (differentiation of peak intensity by temperature) of observed vibration bands on USY. The digits show the wavenumbers of bands. The height of profile is normalized by the maximum value.

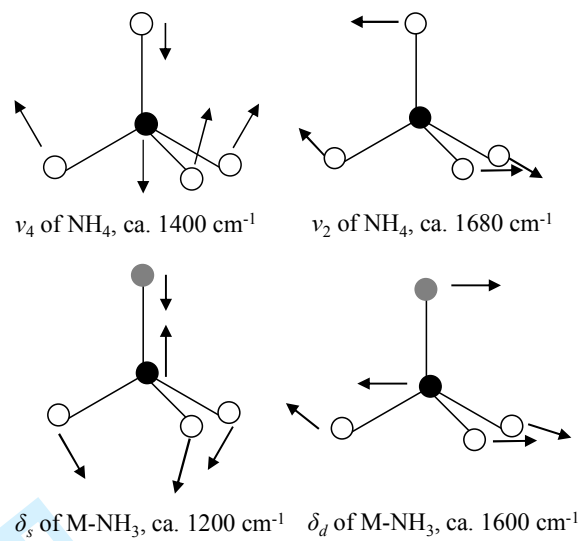
Figure 6: Difference IR spectra [(spectrum measured after the ammonia only adsorption or after adsorption and evacuation)-(spectrum measured at 673 K under vacuum after pre-treatment)] of MOR zeolite recorder at each evacuation time.

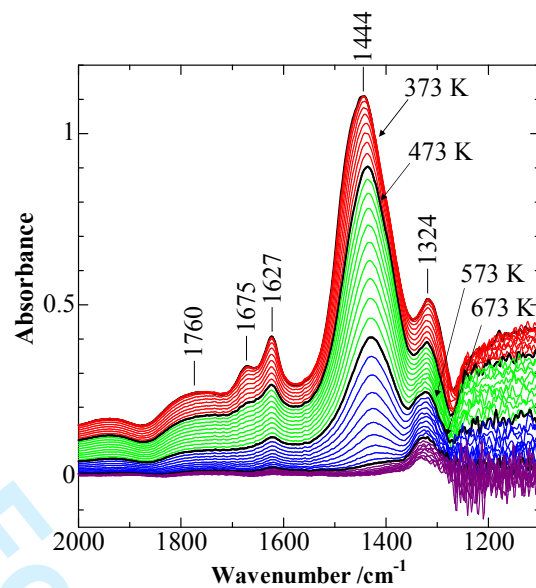
1
2
3
4 Figure 7: Optimized structure of Entry 3, $\text{H}_3\text{N} \rightarrow \text{Al}(\text{OH})_3$.
5
6
7

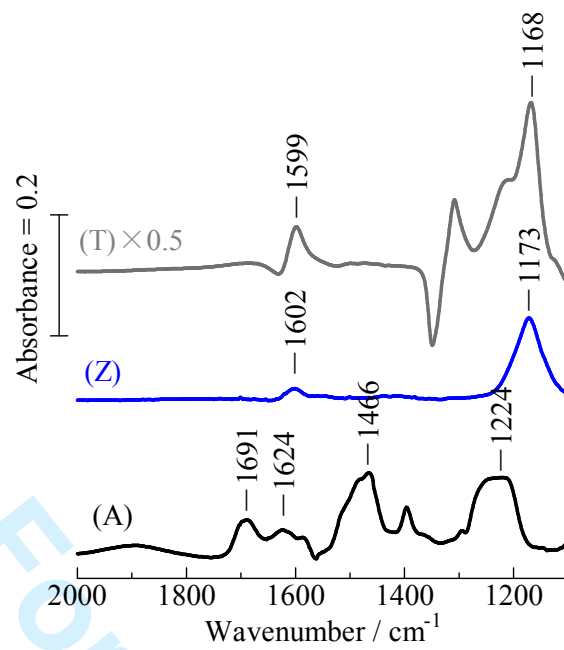
8 Figure 8: Optimized structure of Entry 4, $\text{H}_3\text{N} \cdots \text{H}-\text{O}-\text{Si}(\text{OH})_3$.
9
10

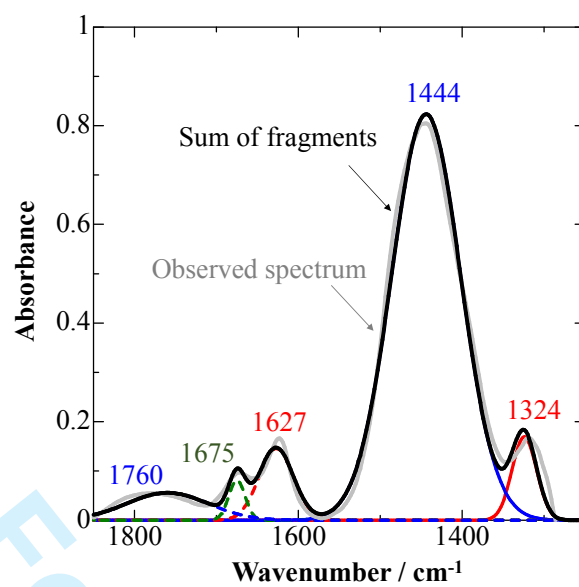
11
12 Figure 9: Estimated TPD profiles from corresponding species on USY zeolite. MS shows the
13 profile of ammonia desorption measured by MS.
14
15
16
17
18
19
20
21
22
23
24
25
26
27
28
29
30
31
32
33
34
35
36
37
38
39
40
41
42
43
44
45
46
47
48
49
50
51
52
53
54
55
56
57
58
59
60

For Peer Review

**Figure 1**

**Figure 2**

**Figure 3**

**Figure 4**

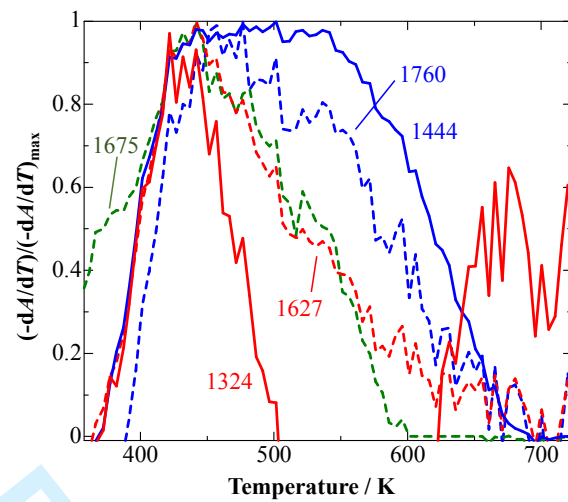
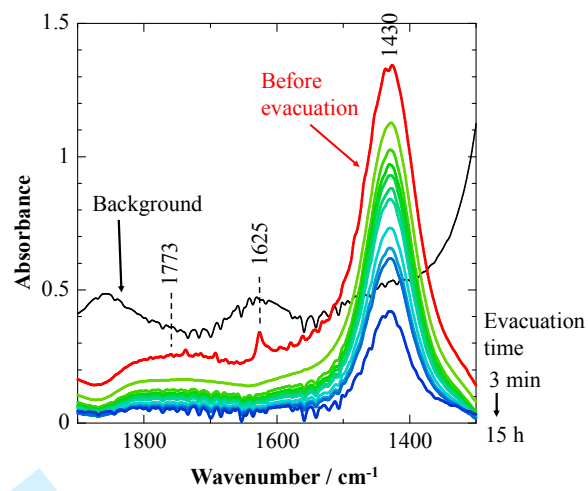


Figure 5

**Figure 6**

1
2
3
4
5
6
7
8
9
10
11
12
13
14
15
16
17
18
19
20
21
22
23
24
25
26
27
28
29
30
31
32
33
34
35
36
37
38
39
40
41
42
43
44
45
46
47
48
49
50
51
52
53
54
55
56
57
58
59
60

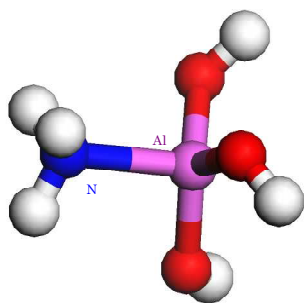
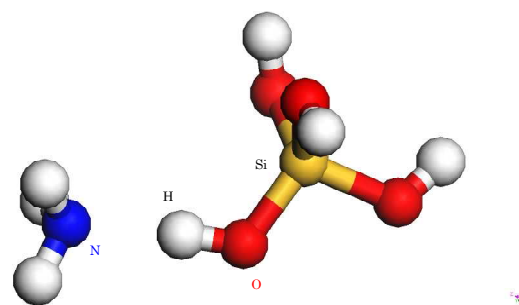
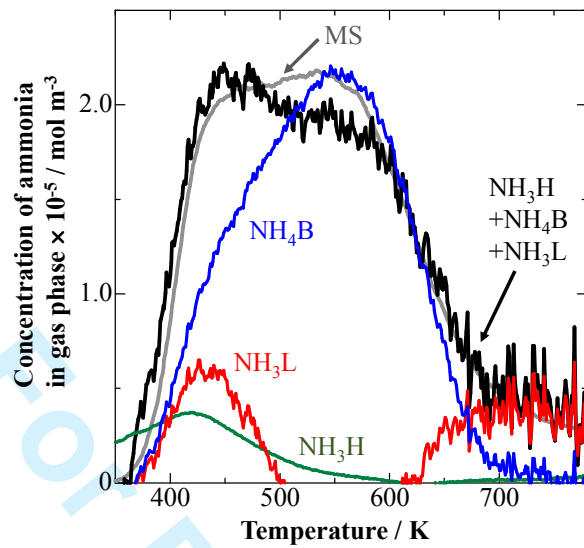


Figure 7

For Peer Review

**Figure 8**

For Peer Review

**Figure 9**

Graphical abstract

Assignments of Bending Vibrations of Ammonia Adsorbed on Solid Surfaces

S. Suganuma*, Y. Murakami, J. Ohyama, T. Torikai, K. Okumura, and N. Katada

Bending vibration bands in infrared (IR) spectra of ammonia adsorbed on Brønsted and Lewis acid sites, and hydrogen-bonded species were assigned with an aid of density functional theory.

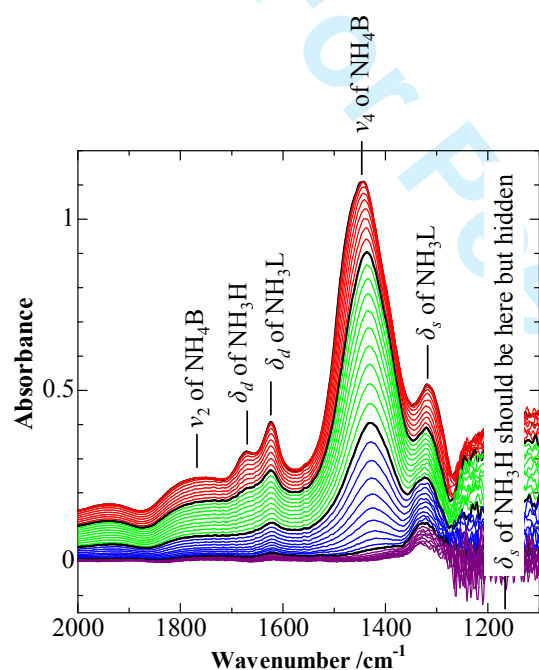


Table 1 Employed oxide samples

Description	Origin
Al ₂ O ₃	Reference catalyst JRC-ALO6 supplied by Reference Catalyst Division, Catalysis Society of Japan, as received
ZrO ₂	Hydrolysis of Zr(ONO ₃) ₂ with NH ₄ OH in an aqueous solution followed by calcination at 773 K for 4 h
TiO ₂	Hydrolysis of Ti[OCH(CH ₃) ₂] with H ₂ O in ethanol followed by calcination at 773 K for 4 h [8]
USY	Small particles (diameter < 50 nm) of USY prepared from a commercial sample of NaY zeolite (HSZ-320NAA from Tosoh, SiO ₂ /Al ₂ O ₃ = 5.5) by ion-exchange with NH ₄ NO ₃ , steaming at 823 K with H ₂ O (18 mol%) / N ₂ and treatment with NH ₄ NO ₃ at 353 K [9]
MOR	Ion-exchange of JRC-Z-M15 with Si/Al ₂ = 15 (Reference catalyst, Reference Catalyst Division, Catalysis Society of Japan) with NH ₄ NO ₃ at 353 K.

Table 2 Calculated and observed wavenumbers. All the calculations have been corrected by multiplying with 0.9630, because the OH stretching wavenumber was calculated to be 3798 cm^{-1} under the same conditions while it was observed at 3657 cm^{-1} .

Entry	Description	Wavenumber (cm^{-1}) of			
		δ_s (NH_3) or ν_4 (NH_4)		δ_d (NH_3) or ν_2 (NH_4)	
		calc.	obs.	calc.	obs.
1	$\text{H}_3\text{N} \rightarrow \text{Al}(\text{OH})_3$	1206	1224 ^a	1602, 1617	1624 ^a
	$\text{H}_3\text{N}/\text{Al}_2\text{O}_3$	1226	1224	1593, 1606	1624
2	$\text{H}_3\text{N} \rightarrow \text{Zr}(\text{OH})_4$	1134	1173 ^b	1566, 1602	1602 ^b
3	$\text{H}_3\text{N} \rightarrow \text{Ti}(\text{OH})_4$	1154	1168 ^c	1592, 1630	1599 ^c
	$\text{H}_3\text{N}/\text{TiO}_2$	1156	1168	1613, 1653	1599
4	$\text{H}_3\text{N} \cdots \text{H}-\text{O}-\text{Si}(\text{OH})_3$	1123		1601, 1615	
5	Free NH_3	1050	1084	1607, 1634	1627
6	$\text{NH}_4 \cdots \text{FAU}$	1319, 1436, 1495	1450 ^d	1640, 1675	1674, 1774
7	$\text{NH}_4 \cdots \text{BEA}$	1344, 1472, 1511	1450 ^d	1673, 1686	1698
8	$\text{NH}_4 \cdots \text{MFI}$	1345, 1473, 1500	1450 ^d	1675, 1676	
9	$\text{NH}_4 \cdots \text{MOR}$		1450 ^d		1582, 1804
10	Free NH_4^+	1430, 1444, 1473		1681, 1694	

a: Observed on Al_2O_3 . b: Observed on ZrO_2 . c: Observed on TiO_2 . d: It looks that a broad band was formed from peaks at 1395, 1445 and 1490 cm^{-1} .

Table 3 Final coordinates of entry 1, $\text{H}_3\text{N} \rightarrow \text{Al}(\text{OH})_3$ (Å)

ID	ATOM	X	Y	Z
1	N	-4.081580	0.773485	-0.684991
2	Al	-2.421710	-0.000899	0.261624
3	O	-1.463078	1.461537	0.385450
4	O	-1.945003	-1.183342	-0.940260
5	O	-3.209663	-0.585120	1.715469
6	H	-3.895919	1.721776	-1.025207
7	H	-4.871509	0.813296	-0.033480
8	H	-4.352062	0.192178	-1.483844
9	H	-3.068668	-1.504843	1.985993
10	H	-1.036146	-1.165325	-1.275970
11	H	-1.152732	1.738705	1.260736

Table 4 Final coordinates of entry 2, $\text{H}_3\text{N} \rightarrow \text{Zr}(\text{OH})_4$ (Å)

ID	ATOM	X	Y	Z
1	N	-4.168566	0.747810	-1.088112
2	Zr	-2.223629	0.445466	0.507362
3	O	-1.337929	0.855829	-1.268799
4	O	-2.900826	-1.442372	0.656379
5	H	-3.997108	1.611308	-1.610041
6	H	-5.080284	0.836977	-0.633345
7	H	-4.219785	-0.011671	-1.771089
8	H	-3.409282	-1.952950	1.302386
9	H	-0.375092	0.954185	-1.350894
10	O	-0.632334	0.427492	1.721550
11	O	-3.288680	1.931244	1.395828
12	H	-2.968697	2.375267	2.199095
13	H	-0.117290	-0.222984	2.217786

Table 5 Final coordinates of entry 3, $\text{H}_3\text{N}\rightarrow\text{Ti}(\text{OH})_4$ (Å)

ID	ATOM	X	Y	Z
1	N	-4.092437	0.693477	-1.075752
2	Ti	-2.278168	0.467780	0.460448
3	O	-1.374531	0.803940	-1.160820
4	O	-2.836046	-1.306636	0.670554
5	H	-4.293349	1.691254	-1.178703
6	H	-4.956200	0.223519	-0.796682
7	H	-3.804529	0.330606	-1.987766
8	H	-3.312982	-1.616478	1.459563
9	H	-0.413361	0.939213	-1.078482
10	O	-0.836793	0.534933	1.653737
11	O	-3.256497	1.859914	1.266797
12	H	-2.848851	2.216879	2.077195
13	H	-0.415759	-0.282800	1.968012

Table 6 Final coordinates of entry 4: $\text{H}_3\text{N}\cdots\text{H}_a\text{-O-Si}(\text{OH})_3$ (Å)

ID	ATOM	X	Y	Z
1	N	-3.149728	1.931289	3.646233
2	Si	-2.145739	-0.054356	0.422084
3	O	-0.687346	0.748297	0.516893
4	O	-2.609491	-0.289966	-1.153493
5	O	-1.808672	-1.499749	1.203879
6	H	-2.478569	2.703158	3.620246
7	H	-4.046269	2.324543	3.943574
8	H	-2.843868	1.294843	4.386341
9	H	-2.555336	-2.118869	1.261648
10	H	-1.916167	-0.649890	-1.730019
11	H	0.013948	0.231239	0.947003
12	O	-3.394994	0.777003	1.062552
13	H	-3.281645	1.152197	1.982249

Table 7 Final coordinates of entry 5, free NH₃ (Å)

ID	ATOM	X	Y	Z
1	N	-0.010477	-0.014395	0.024595
2	H	-0.316066	-0.446786	-0.852060
3	H	-0.315673	0.961076	-0.039395
4	H	1.010932	0.022475	-0.039001

Table 8 Final coordinates of entry 6, free NH₄⁺ (Å)

ID	ATOM	X	Y	Z
1	N	-0.034779	-0.005575	0.000586
2	H	-0.313716	-0.461686	-0.881707
3	H	-0.324085	0.984404	-0.017597
4	H	0.989452	-0.062860	0.108671
5	H	-0.491362	-0.481867	0.793339